Higher-angular-momentum states of the helium atom in a strong magnetic field

W. Becken and P. Schmelcher
Theoretische Chemie, Physikalisch-Chemisches Institut, Im Neuenheimer Feld 229, 69120 Heidelberg, Federal Republic of Germany
(Received 29 September 2000; revised manuscript received 16 January 2001; published 17 April 2001)

A considerable number of higher-angular-momentum states of the helium atom embedded in a magnetic field $B=0-100$ a.u. are investigated using a full configuration-interaction approach which is based on a nonlinearly optimized anisotropic Gaussian basis set of one-particle functions. Spin singlet and triplet states with positive- and negative-z parity are considered for the magnetic quantum number $M=\pm 2$ and positive-z parity states are studied for $M=\pm 3$. Many of the excitations within these symmetries are investigated here. Total energies, ionization energies, as well as transition wavelengths as a function of the field strength are given. A list of stationarities with respect to the field strength which are of immediate interest to astrophysical applications is available.

DOI: 10.1103/PhysRevA.63.053412 PACS number(s): 32.60.+i

I. INTRODUCTION

Strong magnetic fields are well known to severely change the structure and dynamics of atomic and molecular systems. Particularly they enrich the bound-state properties that have in a unique way been demonstrated for the hydrogen atom in a magnetic field [1,2]. Indeed, the theoretical description of atoms in strong magnetic fields is well covered in the literature only for the case of the hydrogen atom (see Refs. [1–7] and references therein). This is in contrast to the astrophysical need of explaining spectra originating from the surfaces of white dwarfs ($\leqslant 10^5$ Tesla) and neutron stars ($\approx 10^8$ Tesla). Through the steadily increasing availability of observatories with higher resolutions and sensitivities more and more objects are discovered with an amazing variety of properties and spectral decompositions [8].

Until recently our knowledge about atoms with more than one electron in a strong magnetic field has been relatively sparse. For a detailed overview of the various theoretical approaches to, for example, the helium atom in a strong magnetic field and the corresponding literature before 1998, we refer the reader to [9] and in particular the references therein. It is only from 1998 on that a major theoretical investigation of the spectrum of two-electron systems became feasible [9,10]: many excited states of different symmetries could be investigated for a broad range of field strengths and, importantly, with a high accuracy required by a comparison with astrophysical observations. As a consequence strong evidence arose that the mysterious absorption edges of the magnetic white dwarf GD229 [11–13], which were for almost 25 years unexplained, are due to helium in a strong magnetic field [14]. This evidence is based on the results of highly accurate *ab initio* calculations that were published in Refs. [9,10] and that apply a fully correlated configuration-interaction approach to the helium atom in a strong magnetic field. Total energies for spin singlet and triplet states for both positive- and negative-z parity for the magnetic quantum numbers $M=0,\pm 1$ have been provided, thereby covering the regime of magnetic-fields strengths from $B=0$ to $B=100$ a.u. ($B=1$ a.u. corresponds to 2.35×10^5 Tesla). Additionally all the transition energies within the $M=0,\pm 1$ subspaces have been presented and discussed there, including the stationary components with respect to the field dependence which have been the key tool for the comparison with the observed spectra [14].

The aim of the present paper is to provide important results for higher excited states with the magnetic quantum numbers $M=\pm 2,\pm 3$ thereby covering the spin singlet and triplet symmetries as well as positive- and negative-z parities for $M=\pm 2$ and positive-z parities for $M=\pm 3$. Thereby we will obtain new insights into a largely unknown part of the spectrum and reveal some interesting and appealing binding mechanisms of the atom in the field. Of course, the resulting data are indispensable to completing the picture of the energetics of the atom, i.e., to extending our knowledge on the helium atom in a strong magnetic field: They permit us to investigate additional transitions and allow us to solidify a comparison with astronomical observation. As indicated above little is known in the literature about the states investigated here. For the case of triplet spin symmetry, Jones and Ortiz [15] very recently used a released-phase quantum Monte Carlo method for calculating a few accurate data. However, they cover only three field strengths, investigate much less excited states, and do not study the spin singlet states at all. Nevertheless, as we shall see, for the common values of the field strength they coincide with our data to several digits.

We emphasize that major extensions of our previous computational method were necessary in order to perform the calculations for higher magnetic quantum numbers: the multiple summation techniques as well as the implementation of the higher transcendental functions had to be improved substantially (see for comparison Ref. [10]) in order to ensure an affordable CPU for the evaluation of the numerous electron-electron integrals and consequently the Hamiltonian matrix. Including these improvements the CPU involved in the present work amounts to 9 months on a fast workstation.

The starting point of the present paper is the nonrelativistic Hamiltonian of the helium atom with infinite nuclear mass in a magnetic field as given in Sec. II. To be self-contained we briefly discuss the Hamiltonian's symmetries and provide a description of the basis set as well as the full configuration-interaction approach (for more details see Ref. [9]). We introduce a maximal set of conserved quantities, chosen to be the total spin S^2, the z component S_z of the total spin, the total spatial magnetic quantum number M, and the

TABLE I. Correspondence table of higher excited states of the helium atom: field-free ($B=0$) spectroscopic notation is $n^{2S+1}L_M$ and field notation ($B\neq 0$) is $\nu^{2S+1}M^{\Pi_z}$. The upper two (double) rows contain the singlet states and the lower two (double) rows the triplet states. The singlet and triplet states are ordered with increasing energy, respectively. States in between two vertical double lines are energetically degenerate.

$B=0$ $(n^{2S+1}L_M)$	$6^1D_{\pm 2}$	$6^1F_{\pm 2}$	$6^1F_{\pm 3}$	$6^1G_{\pm 2}$	$6^1G_{\pm 3}$	$6^1H_{\pm 2}$	$6^1H_{\pm 3}$
$B\neq 0$ $(\nu^{2S+1}M^{\Pi_z})$	$5^1(\pm 2)^+$	$3^1(\pm 2)^-$	$3^1(\pm 3)^+$	$6^1(\pm 2)^+$	$2^1(\pm 3)^-$	$4^1(\pm 2)^-$	$4^1(\pm 3)^+$
$B=0$ (n^{2S+1L_M})	$7^1D_{\pm 2}$	$7^1F_{\pm 2}$	$7^1F_{\pm 3}$	$7^1G_{\pm 2}$	$7^1G_{\pm 3}$	$7^1H_{\pm 2}$	$7^1H_{\pm 3}$
$B\neq 0$ $(\nu^{2S+1}M^{\Pi_z})$	$7^1(\pm 2)^+$	$5^1(\pm 2)^-$	$5^1(\pm 3)^+$	$8^1(\pm 2)^+$	$3^1(\pm 3)^-$	$6^1(\pm 2)^-$	$6^1(\pm 3)^+$
$B=0$ $(n^{2S+1}L_M)$	$6^3D_{\pm 2}$	$6^3F_{\pm 2}$	$6^3F_{\pm 3}$	$6^3G_{\pm 2}$	$6^3G_{\pm 3}$	$6^3H_{\pm 2}$	$6^3H_{\pm 3}$
$B\neq 0$ $(\nu^{2S+1}M^{\Pi_z})$	$5^3(\pm 2)^+$	$3^3(\pm 2)^-$	$3^3(\pm 3)^+$	$6^3(\pm 2)^+$	$2^3(\pm 3)^-$	$4^3(\pm 2)^-$	$4^3(\pm 3)^+$
$B=0$ $(n^{2S+1}L_M)$	$7^3D_{\pm 2}$	$7^3F_{\pm 2}$	$7^3F_{\pm 3}$	$7^3G_{\pm 2}$	$7^3G_{\pm 3}$	$7^3H_{\pm 2}$	$7^3H_{\pm 3}$
$B\neq 0$ $(\nu^{2S+1}M^{\Pi_z})$	$7^3(\pm 2)^+$	$5^3(\pm 2)^-$	$5^3(\pm 3)^+$	$8^3(\pm 2)^+$	$3^3(\pm 3)^-$	$6^3(\pm 2)^-$	$6^3(\pm 3)^+$

total spatial z parity Π_z. These symmetries serve for classifying the results for the energies for $M=\pm 2,\pm 3$ in Sec. III. In each of the subspaces for positive- and negative-z parity we present the total energies and the ionization energies of the ground state and the first four excited states for singlet and triplet spin symmetry. Additionally we consider in Sec. IV all the transitions involving the $M=\pm 2,\pm 3$ subspaces. The wavelengths of the stationary components, which are the basic ingredients for the successful comparison of theoretical data with the spectra of magnetic white dwarfs in general, are available.

II. HAMILTONIAN, SYMMETRIES, AND BASIS SETS

A. Hamiltonian and symmetries

Assuming the magnetic field to point in the positive-z direction, the Hamiltonian reads in atomic units

$$H=\sum_{i=1}^{2}\left(\frac{1}{2}\mathbf{p}_i^2+\frac{1}{2}Bl_{zi}+\frac{B^2}{8}(x_i^2+y_i^2)-\frac{2}{|\mathbf{r}_i|}+Bs_{zi}\right)+\frac{1}{|\mathbf{r}_2-\mathbf{r}_1|}. \quad (1)$$

The one-particle operators in Eq. (1) are the Coulomb potential energies $-2/|\mathbf{r}_i|$ of the electrons in the field of the nucleus as well as their kinetic energies, here split into the parts $\frac{1}{2}\mathbf{p}_i^2$, the Zeeman terms $\frac{1}{2}Bl_{zi}$, the diamagnetic terms $(B^2/8)(x_i^2+y_i^2)$ and their spin energies Bs_{zi}. The electron-electron repulsion energy is represented by the two-particle operator $1/|\mathbf{r}_2-\mathbf{r}_1|$. We use an electron spin g factor equal to 2. Any more accurate values for it can be simply incorporated by shifting the final total energies correspondingly. For remarks on the influence of relativistic effects and on a scaling relation taking into account the finite nuclear mass, we refer the reader to Refs. [2,9,16].

Analogously to Ref. [9], we exploit that there exist four independent commuting conserved quantities: the total spin $\mathbf{S}^2$, the z component S_z of the total spin, the z component L_z of the total angular momentum, and the total spatial z parity Π_z. Throughout the paper we use the notation $\nu_{S_z}^{2S+1}M^{(-1)^{\Pi_z}}$ for a state with spin multiplicity $(2S+1)$ and the degree of excitation $\nu=1,2,3,...$ within the subspace of a given magnetic quantum number M and z parity Π_z. The index S_z will be omitted in obvious cases. The present paper investigates the subspaces $^1(\pm 2)^+$, $^3(\pm 2)^+$, $^1(\pm 2)^-$, $^3(\pm 2)^-$, as well as the two symmetries $^1(\pm 3)^+$, $^3(\pm 3)^+$. The correspondence between our field notation and the common spectroscopic notation $n_{S_z}^{2S+1}L_M$ in field-free space is discussed in Ref. [9] (see Table I therein) up to the fourth field-free excitation of a certain symmetry. However, the present results exceed this degree of excitation and Table I in the present paper therefore provides the correspondence for the fifth and sixth excitations.

B. Basis set, optimization, and the configuration-interaction approach

For constructing a two-particle basis set of eigenfunctions of the above-mentioned conserved quantities, our central ingredient is an anisotropic Gaussian basis set of one-particle functions

$$\Phi_i(\rho,\varphi,z)=\rho^{n_{\rho i}}z^{n_{zi}}e^{-\alpha_i\rho^2-\beta_i z^2}e^{im_i\varphi}, \quad i=1,...,n, \quad (2)$$

which are themselves eigenfunctions of the corresponding one-particle operators of the mentioned conserved quantities. The parameters $n_{\rho i}$ and n_{zi} are restricted by

$$n_{\rho_i}=|m_i|+2k_i, \quad k_i=0,1,2,... \quad \text{with} \quad m_i=...-2,-1,0,1,2,..., \quad (3)$$

$$n_{zi}=\pi_{zi}+2l_i, \quad l_i=0,1,2,... \quad \text{with} \quad \pi_{zi}=0,1, \quad (4)$$

whereas the nonlinear variational parameters α_i and β_i are positive and have to be nonlinearly optimized for each field strength as described in Ref. [9]. For each one-particle subspace of given symmetry we used the pattern search method to determine the nonlinear parameters α_i and β_i such that the states of the hydrogen atom or the He^+ ion for that symmetry were optimally described. We emphasize that this procedure gives rise to considerable effort since it has to be repeated for each field strength separately.

We construct a basis set of spatial two-particle states by

TABLE II. Total energies E of the ground and first four excited singlet states $\nu^1(-2)^+$, $\nu=1-5$ as a function of the magnetic field strength B. The values for $B=0$ given in the literature are included. No values for finite field strength are available in the literature for comparison. The last column $T(B)$ defines the ionization threshold.

B	$E(1^1(-2)^+)$	$E(2^1(-2)^+)$	$E(3^1(-2)^+)$	$E(4^1(-2)^+)$	$E(5^1(-2)^+)$	T
0.000	−2.055 619	−2.031 279	−2.020 015	−2.020 000	−2.013 897	−2.000 000 000
	−2.055 620 7[a]	−2.031 279 8[a]	−2.020 015 8[a]	−2.020 000 7[a]	−2.013 898[a]	
0.0008	−2.056 410	−2.032 044	−2.020 763	−2.020 721	−2.014 589	−1.999 599 960
0.004	−2.059 404	−2.034 441	−2.023 111	−2.021 874	−2.015 860	−1.997 999 000
0.008	−2.062 771	−2.036 156	−2.024 819	−2.020 841	−2.015 821	−1.995 995 995
0.020	−2.070 739	−2.036 364	−2.025 499	−2.015 103	−2.009 601	−1.989 975 001
0.040	−2.079 134	−2.031 460	−2.018 544	−2.008 093	−1.999 079	−1.979 900 008
0.080	−2.086 450	−2.019 554	−1.995 169	−1.985 820	−1.980 016	−1.959 600 176
0.160	−2.084 575	−1.990 063	−1.957 535	−1.942 694	−1.934 690	−1.918 402 804
0.240	−2.072 379	−1.956 003	−1.918 410	−1.901 981	−1.893 298	−1.876 414 090
0.400	−2.032 455	−1.880 602	−1.835 877	−1.817 352	−1.807 742	−1.790 105 922
0.500	−2.000 873	−1.830 171	−1.782 074	−1.762 605	−1.752 984	−1.734 628 064
0.800	−1.886 749	−1.668 200	−1.612 514	−1.591 024	−1.580 675	−1.561 526 260
1.0	−1.798 936	−1.553 161	−1.493 657	−1.471 195	−1.460 424	−1.440 989 741
1.6	−1.497 199	−1.182 567	−1.114 605	−1.090 086	−1.078 557	−1.058 421 519
2.0	−1.272 473	−0.918 836	−0.846 682	−0.821 183	−0.809 329	−0.788 842 154
5.0	0.734 276	1.301 338	1.391 631	1.421 128	1.434 251	1.456 132 354
10.0	4.636 327	5.435 657	5.540 419	5.572 921	5.587 127	5.609 851 957
20.0	13.174 417	14.283 868	14.403 805	14.439 449	14.454 604	14.478 404 53
50.0	40.558 628	42.224 693	42.364 599	42.405 944	42.424 321	42.453 697 55
100.0	87.949 762	91.119 604	90.256 267	90.363 401	90.399 817	90.439 453 48

[a]Drake and Yan [17].

$$|\psi_q\rangle := b_i^\dagger b_j^\dagger |0\rangle, \quad i=1,...,n, \quad j=i,\ldots,n, \tag{5}$$

where $b_i^\dagger$ is the creation operator of the ith one-particle state $|i\rangle = b_i^\dagger|0\rangle$ whose position representation is given by Eq. (2). The spin space is spanned by spin singlet or spin triplet states, and therefore the operators $b_i^\dagger$ have to be chosen bosonic or fermionic, respectively. Selecting combinations with

$$m_i + m_j = M, \quad \mathrm{mod}(\pi_{zi}+\pi_{zj},2) = \Pi_z, \tag{6}$$

we achieve the two-particle states (5) to be a basis set within the subspace for given total symmetries M and Π_z. The number N of two-particle basis states is thus in general smaller then $n(n+1)/2$.

We perform a *full configuration-interaction* (full CI) approach by representing the Hamiltonian in a basis whose spatial part is given by the in general nonorthonormal states (5). Since the spin part $B\Sigma s_{zi}$ of the Hamiltonian can trivially be taken into account by a shift of the energies it is sufficient to represent the spatial part of the Hamiltonian H and the overlap S by

$$S_{pq} = \langle\psi_p|\psi_q\rangle, \quad H_{pq} = \langle\psi_p|H|\psi_q\rangle. \tag{7}$$

The matrices S and H are Hermitian, and the overlap S is additionally positive definite. Furthermore, the matrix elements turn out to be real. The finite-dimensional generalized real-symmetric eigenvalue problem

$$(H - ES)\cdot c = 0 \tag{8}$$

provides eigenvalues E that are variational upper bounds to the exact eigenvalues of the Hamiltonian (1) within each subspace of given M and Π_z.

C. Matrix elements

For calculating the matrix elements of the spatial part of the Hamiltonian (1), we rewrite the former in second quantization, $\hat{H} = \hat{H}_\mathrm{I} + \hat{H}_\mathrm{II}$, where $\hat{H}_\mathrm{I}$ and $\hat{H}_\mathrm{II}$ denote the second-quantized counterparts of the familiar one- and two-particle operators whose position representations read

$$H_\mathrm{I}(\mathbf{p},\mathbf{r}) = \frac{1}{2}\mathbf{p}^2 + \frac{1}{2}\mathbf{B}\cdot\boldsymbol{l} + \frac{1}{8}B^2(x^2+y^2) - \frac{2}{|\mathbf{r}|},$$

$$H_\mathrm{II}(\mathbf{r}_1,\mathbf{r}_2) = \frac{1}{|\mathbf{r}_2-\mathbf{r}_1|}. \tag{9}$$

Now, with $|\psi_q\rangle := b_i^\dagger b_j^\dagger|0\rangle$ and $|\psi_p\rangle := b_k^\dagger b_l^\dagger|0\rangle$ a straightforward calculation leads to

$$\langle\psi_p|\psi_q\rangle = \langle i|k\rangle\langle j|l\rangle \pm \langle i|l\rangle\langle j|k\rangle, \tag{10}$$

$$\langle\psi_p|\hat{H}_\mathrm{I}|\psi_q\rangle = \langle i|H_\mathrm{I}|k\rangle\langle j|l\rangle \pm \langle i|H_\mathrm{I}|l\rangle\langle j|k\rangle + \langle j|H_\mathrm{I}|l\rangle\langle i|k\rangle \pm \langle j|H_\mathrm{I}|k\rangle\langle i|l\rangle, \tag{11}$$

$$\langle\psi_p|\hat{H}_\mathrm{II}|\psi_q\rangle = \langle ij|H_\mathrm{II}|kl\rangle \pm \langle ij|H_\mathrm{II}|lk\rangle, \tag{12}$$

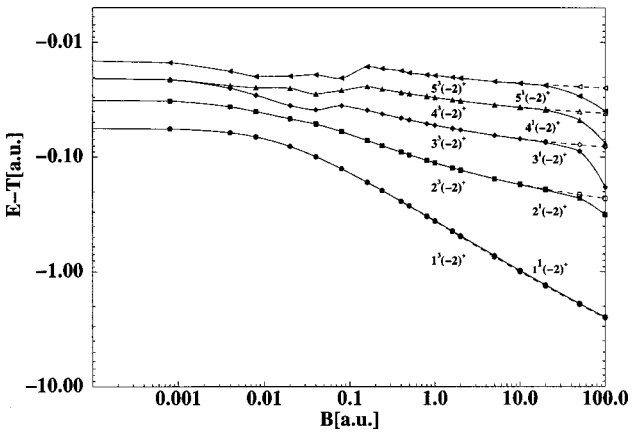

FIG. 1. The ionization energies of the ground and first four excited states $\nu^{2S+1}(-2)^+$ for both singlet ($S=0$) (solid lines) and triplet ($S=1$) (broken lines) symmetry as a function of the field strength. In most cases, i.e., for a broad range of field strengths, the singlet-triplet splitting is very small. Both energies and field strengths are given in atomic units.

where $|ij\rangle := |i\rangle \otimes |j\rangle$ and where the sign ''$\pm$'' stands for ''$+$'' in the singlet case and for ''$-$'' in the triplet case.

For the relatively simple evaluation of the $n(n+1)/2$ different one-particle overlaps $\langle i/k\rangle$ and matrix elements $\langle i|H_{\mathrm{I}}|k\rangle$ we refer the reader to Appendixes *A* and *B* in Ref. [9]. In contrast the two-particle matrix elements $\langle ij|H_{\mathrm{II}}|kl\rangle$ are by no means trivial, particularly in view of the fact that their accurate and fast evaluation is necessary in order to build up the Hamiltonian matrix in an affordable amount of CPU time. In Ref. [9] we discussed a method using a decomposition in Cartesian coordinates that expresses the two-particle matrix elements in a series of hypergeometric functions whose evaluation has been performed by highly efficient analytical continuation formulas. The latter are necessary in order to keep the CPU time acceptable since the number of different two-particle matrix elements is of the order $N(N+1)/2$ rather than $n(n+1)/2$. However, the Cartesian decomposition becomes more and more inefficient with increasing magnetic quantum number, which is already relevant for calculations of the subspace $M=-1$ and indispensable for the present work ($|M|=2,3$). Therefore a drastically improved technique using cylindrical coordinates has been developed and described in Ref. [10]. This leads to an enormous gain of speed such that the computation of the whole Hamiltonian matrix becomes even faster than its diagonalization by standard library routines. The derivation of the corresponding powerful formula for the electron-electron integral is rather lengthy and complicated and we refer the reader to Appendixes A, B, and C of Ref. [10] for the illustration of the corresponding major steps.

D. Aspects for the selection of basis functions

For the $M=0$ states treated in Ref. [9] we have been able to achieve a considerable accuracy by choosing basis sets that can describe the shape of the exact wave function, i.e., include electronic correlation effects. The latter becomes less important with increasing quantum number $|M|$, and this manifests itself particularly for the present values $M=\pm 2$, ± 3. The reason is that bound two-particle states with nonzero values of M are approximately one-particle excitations. Consequently, the electrons are spatially more separated than in a 0^+ state, and this lowers the correlation energy. Additionally, the cusp problem is also less important for excited states $M\neq 0$, and therefore fewer one-particle functions with large values for the nonlinear α and β parameters are needed. We have exploited these facts and achieved even more accurate results for the $M\neq 0$ states than for the $M=0$ states.

In detail our strategy was similar to the $M=0$ case. We used of the order of 200 optimized one-particle basis functions (for each field strength) to construct a two-particle basis set containing 3000 to 4000 configurations. In order to describe angular correlation, we have also included configurations for which both electrons possess a nonzero angular momentum. This was done for both positive- and negative-z parities, although for negative-z parity less such configurations are needed to achieve the same accuracy. In order to describe the excitations properly we added a significant number of one-particle basis functions with quantum numbers l_i, $k_i\neq 0$ [see Eqs. (3) and (4)]. The latter have exclusively been optimized for a nuclear charge number $Z=1$, in contrast to all the other types of basis functions that have been optimized for $Z=1$ (hydrogen) and for $Z=2(\mathrm{He}^+)$. In the following we present and discuss our results for the higher excited states $M=\pm 2,\pm 3$ of the helium atom.

III. RESULTS AND DISCUSSION

A. Total and ionization energies

We investigate the total and one-particle ionization energies of higher excited states of the helium atom according to the following sequence of symmetries $^1(-2)^+$, $^3(-2)^+$, $^1(-2)^-$, $^3(-2)^-$, $^1(-3)^+$, $^3(-3)^+$. Within each of these subspaces five electronic states will be studied. The total energies E are defined to be the eigenvalues of the total Hamiltonian excluding the spin Zeeman term. They will be provided for the above-mentioned 12 symmetries, i.e., the energies of a total of 30 states will be given in table form for a grid of 20 field strengths in the regime $0\leqslant B\leqslant 100$ a.u. which covers in particular the regime of strong fields of magnetic white dwarfs. A comparison with the few data available in the literature will be performed. The one-particle ionization energy E_i is a sensitive quantity that reflects the internal energetics of the atom and refers to the process $\mathrm{He}\rightarrow\mathrm{He}^+ + e$. It is defined as $E_i=|E(B)-T(B)|$, where $T(B)$ is the threshold energy, i.e., the lowest possible total energy for which the system $\mathrm{He}^+ + e$ exists, respecting the symmetries. The values for $T(B)$ are given in the last column of Table II. E_i, in contrast to E, is not masked by the zero-point energy in the external field which is linearly increasing with increasing field strength. The ionization energies are illustrated graphically.

1. The subspace $M=-2$ and even-z parity

The total energies for the singlet subspace are presented in Table II. The only values available in the literature for all

TABLE III. Total energies E of the ground and first four excited triplet states $\nu^3(-2)^+$, $\nu=1-5$ as a function of the magnetic field strength B. The best values E_{lit} available in the literature are included for comparison. For the third and fourth excited state only the energy values for $B=0$ are known so far.

	$1^3(-2)^+$		$2^3(-2)^+$		$3^3(-2)^+$		$4^3(-2)^+$	$5^3(-2)^+$
B	E	E_{lit}	E	E_{lit}	E	E_{lit}	E	E
0.000	−2.055 635	−2.055 636[a]	−2.031 288	−2.031 288 8[a]	−2.020 021	−2.020 021[a]	−2.020 000	−2.013 900
							−2.020 000 7[a]	−2.013 901[a]
0.0008	−2.056 426		−2.032 054		−2.020 764		−2.020 726	−2.014 589
0.004	−2.059 420		−2.034 451		−2.023 111		−2.021 881	−2.015 860
0.008	−2.062 788		−2.036 167		−2.024 820		−2.020 849	−2.015 822
0.020	−2.070 760		−2.036 382		−2.025 502		−2.015 105	−2.009 614
0.040	−2.079 167		−2.031 484		−2.018 564		−2.008 093	−1.999 079
0.080	−2.086 519	−2.0859[b]	−2.019 580	−2.0190[b]	−1.995 202	−1.9942[b]	−1.985 874	−1.980 022
0.160	−2.084 776		−1.990 108		−1.957 557		−1.942 706	−1.934 699
0.240	−2.072 786		−1.956 077		−1.918 439		−1.901 996	−1.893 307
0.400	−2.033 466	−2.0320[b]	−1.880 748	−1.8801[b]	−1.835 928	−1.8356[b]	−1.817 375	−1.807 757
0.500	−2.002 362		−1.830 366		−1.782 138		−1.762 634	−1.752 999
0.800	−1.889 916	−1.8871[b]	−1.668 537	−1.6680[b]	−1.612 616	−1.6120[b]	−1.591 067	−1.580 698
1.0	−1.803 296		−1.553 577		−1.493 778		−1.471 246	−1.460 451
1.6	−1.504 935	−1.5005[b]	−1.183 127	−1.1822[b]	−1.114 753	−1.1141[b]	−1.090 145	−1.078 589
2.0	−1.282 141		−0.919 428		−0.846 828		−0.821 240	−0.809 359
5.0	0.715 950		1.301 189		1.391 674		1.421 157	1.434 268
10.0	4.612 069		5.436 805		5.540 914		5.573 145	5.587 253
20.0	13.145 189		14.287 811		14.405 345		14.440 139	14.454 974
50.0	40.523 943		42.240 836		42.375 670		42.413 590	42.429 456
100.0	87.911 434		90.210 465		90.358 003		90.398 109	90.414 514

[a]Drake and Yan [17].

[b]Jones *et al.* [15].

five states listed are the values for the atom in field-free space. The relative accuracy of our field-free data in comparison with those of Ref. [17] is at least 10^{-6}. We expect this relative accuracy to decrease to some extent with increasing field strength. Although there are no data to compare with in the presence of a strong field we are confident that the accuracy of our total energies is better than a few times 10^{-4} for any field strength. The corresponding ionization energies are shown in Fig. 1 (for reasons of illustration the sign of $[E(B)-T(B)]$ has been included). First we note that the ionization energies of the ground and first excited state increase monotonically with increasing field strength. This does not hold for the higher excited states (second to fourth excited state) which is due to avoided crossings (all states possess the same symmetry) with changing field strength. Such avoided crossings occur in the intermediate regime where the electronic wave function is rearranged and changes its symmetry properties. In the high-field regime $B \gg 1$ a.u. a strictly monotonous behavior is observed for the ionization energies of all five states considered. Clearly the (absolute) increase of the ionization energy with increasing field strength becomes less for the higher excited states.

Turning to the triplet states, Table III provides the total energies for the ground and first four excited states. In contrast to the singlet states there exist some data in the literature on the triplet states for finite field strength: the ground and first two excited states have been studied for a few field strengths in Ref. [15] by first performing Hartree-Fock calculations and then a quantum Monte Carlo simulation to obtain correlated results. The resulting data have been included in Table III for comparison. First of all we remark that, analogous to the singlet states, the accuracy of our energies of the triplet states for $B=0$ is at least 10^{-6} (our field-free energies are always compared with those of Ref. [17]). In the presence of a strong field our values are, depending on the state and field strength, systematically variationally lower by typically $10^{-3}-10^{-4}$ a.u. than those given in Ref. [15]. Again we expect the accuracy of our total energies to be at least of the order of 10^{-4}. According to Fig. 1 the singlet-triplet splitting of the (ionization) energies is generally very small (the solid and broken lines in Fig. 1 are almost indistinguishable). An exception is the behavior of the ionization energies for the excited states in very strong fields $B \geqslant 20$: the singlet ionization energies show a significantly stronger increase compared to the triplet energies in this regime. It is conjectured that this is due to correlation effects in strong fields. The $^1(-2)^+$ subspace allows for configurations which are built of identical one-particle functions possessing the symmetry $(-1)^+$. Obviously these one-particle functions contribute only to the singlet but not to the triplet states which have an antisymmetric spatial wave function. The observed decrease should therefore be characteristic for the subspaces $^1(-2)^+$, $^1(-4)^+$, $^1(-6)^+$, etc., and in particu-

TABLE IV. Total energies E of the ground and first four excited singlet states $\nu^1(-2)^-$, $\nu=1-5$ as a function of the magnetic field strength B. The values for $B=0$ given in the literature are included. No values for finite field strength are available in the literature for comparison.

B	$E(1^1(-2)^-)$	$E(2^1(-2)^-)$	$E(3^1(-2)^-)$	$E(4^1(-2)^-)$	$E(5^1(-2)^-)$
0.000	−2.031 254	−2.020 002	−2.013 890	−2.013 889	−2.010 205
	−2.031 255[a]	−2.020 002 9[a]	−2.013 890 6[a]	−2.013 889 0[a]	−2.010 205 2[a]
0.0008	−2.032 035	−2.020 743	−2.014 622	−2.014 546	−2.010 831
0.004	−2.034 784	−2.022 629	−2.016 384	−2.014 975	−2.011 516
0.008	−2.037 468	−2.023 369	−2.016 833	−2.013 555	−2.010 451
0.020	−2.042 177	−2.022 065	−2.012 876	−2.008 813	−2.004 364
0.040	−2.044 414	−2.017 104	−2.003 883	−1.996 768	−1.993 208
0.080	−2.040 532	−2.003 304	−1.986 398	−1.977 524	−1.972 335
0.160	−2.020 268	−1.969 607	−1.948 470	−1.937 989	−1.932 080
0.240	−1.992 761	−1.932 336	−1.908 453	−1.896 986	−1.890 637
0.400	−1.927 139	−1.852 208	−1.824 627	−1.811 896	−1.804 880
0.500	−1.881 556	−1.799 485	−1.770 222	−1.756 937	−1.749 869
0.800	−1.730 976	−1.632 241	−1.599 339	−1.584 893	−1.577 309
1.0	−1.621 891	−1.514 490	−1.479 829	−1.464 839	−1.456 938
1.6	−1.264 850	−1.137 732	−1.099 353	−1.083 243	−1.074 991
2.0	−1.007 945	−0.870 859	−0.830 725	−0.814 102	−0.805 618
5.0	1.183 243	1.363 685	1.410 696	1.429 264	1.438 506
10.0	5.297 273	5.510 572	5.562 177	5.581 990	5.591 622
20.0	14.129 930	14.373 429	14.428 912	14.449 746	14.459 803
50.0	42.066 688	42.343 038	42.402 428	42.424 265	42.434 671
100.0	90.030 890	90.325 814	90.387 277	90.409 635	90.420 207

[a]Drake and Yan [17].

lar should not occur for the symmetry subspaces with negative-z parity (see below). Furthermore, the energy lowering due to correlation is most pronounced (see Fig. 1) for the intermediate, specifically the second, excited state, which is among others due to the logarithmic scale.

2. The subspace $M=-2$ and odd-z parity

The total energies for the singlet subspace are given in Table IV. Again the only values available in the literature for all five states listed are those for the atom in field-free space. The relative accuracy of our field-free data is at least 10^{-6}. The corresponding ionization energies are shown in Fig. 2. For the ground and first two excited states they increase monotonically with increasing field strength. Avoided crossings in the intermediate regime of field strengths cause the ionization energies of the third and fourth excited state to slightly decrease in the corresponding regime of field strengths. In the high-field regime $B>1$ a.u. a strictly monotonous behavior is observed for the ionization energies of all five states considered. However, in comparison with the subspace $(-2)^+$ there is an overall tendency towards saturation, i.e., the increase of the ionization energies with increasing field strength slows down significantly. The negative-z parity states therefore do not show a significant dependence of their ionization energies on the field strength in the high-field limit. This difference with respect to the increase of the ionization energy for the subspaces $(-2)^+$ and $(-2)^-$ can for the lowest states be attributed to the fact that the excited electron occupies a tightly bound orbital $(3d_{-2})$ in case of the $(-2)^+$ subspace and a nontightly bound orbital for the $(-2)^-$ subspace.

Table V provides the total energies of the corresponding triplet states. Apart from the field-free energy values that possess the same accuracy as discussed above there are a few values for strong fields available in the literature: In Ref. [15] the ground and first two excited states of $^3(-2)^-$ symmetry have been considered. Our energies are systematically variationally lower by an absolute value of $10^{-3}-10^{-4}$ a.u. than those given in Ref. [15]. Similar to the $^3(-2)^+$ subspace the

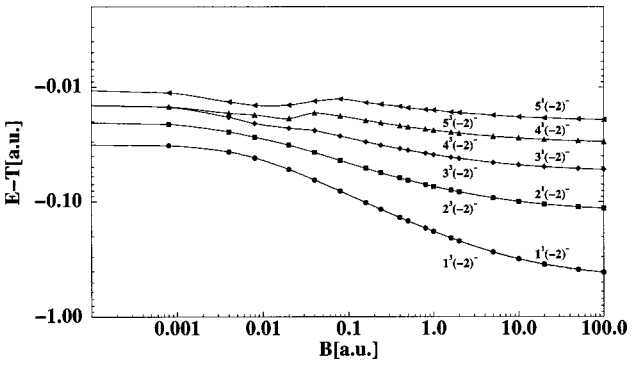

FIG. 2. The ionization energies of the ground and first four excited states $\nu^{2S+1}(-2)^-$ for both singlet ($S=0$) (solid lines) and triplet ($S=1$) (broken lines) symmetry as a function of the field strength. In the considered range of field strengths the singlet-triplet splitting is very small. Both energies and field strengths are given in atomic units.

TABLE V. Total energies E of the ground and first four excited triplet states $\nu^3(-2)^-$, $\nu=1-5$ as a function of the magnetic field strength B. The best values $E_{\rm lit}$ available in the literature are included for comparison. For the third and fourth excited state only the energy values for $B=0$ are known so far.

	$1^3(-2)^-$		$2^3(-2)^-$		$3^3(-2)^-$		$4^3(-2)^-$	$5^3(-2)^-$
B	E	$E_{\rm lit}$	E	$E_{\rm lit}$	E	$E_{\rm lit}$	E	E
0.000	−2.031 254	−2.031 255[a]	−2.020 002	−2.020 002 9[a]	−2.013 890	−2.013 890 6[a]	−2.013 889	−2.010 205
							−2.013 889 0[a]	−2.010 205 2[a]
0.0008	−2.032 035		−2.020 743		−2.014 622		−2.014 546	−2.010 831
0.004	−2.034 784		−2.022 629		−2.016 384		−2.014 975	−2.011 516
0.008	−2.037 468		−2.023 369		−2.016 833		−2.013 555	−2.010 451
0.020	−2.042 177		−2.022 065		−2.012 876		−2.008 813	−2.004 364
0.040	−2.044 414		−2.017 104		−2.003 884		−1.996 768	−1.993 208
0.080	−2.040 532	−2.0401[b]	−2.003 304	−2.0029[b]	−1.986 398	−1.9836[b]	−1.977 524	−1.972 335
0.160	−2.020 271		−1.969 608		−1.948 471		−1.937 989	−1.932 080
0.240	−1.992 769		−1.932 340		−1.908 454		−1.896 987	−1.890 638
0.400	−1.927 166	−1.9268[b]	−1.852 217	−1.8521[b]	−1.824 631	−1.8241[b]	−1.811 898	−1.804 882
0.500	−1.881 601		−1.799 499		−1.770 228		−1.756 940	−1.749 870
0.800	−1.731 094	−1.7299[b]	−1.632 275	−1.6317[b]	−1.599 352	−1.5985[b]	−1.584 899	−1.577 313
1.0	−1.622 067		−1.514 537		−1.479 848		−1.464 848	−1.456 943
1.6	−1.265 215	−1.2637[b]	−1.137 820	−1.1372[b]	−1.099 385	−1.0990[b]	−1.083 259	−1.075 000
2.0	−1.008 432		−0.870 970		−0.830 765		−0.814 120	−0.805 629
5.0	1.182 100		1.363 472		1.410 624		1.429 232	1.438 487
10.0	5.295 577		5.510 289		5.562 085		5.581 949	5.591 600
20.0	14.127 744		14.373 092		14.428 805		14.449 699	14.459 777
50.0	42.064 067		42.342 659		42.402 311		42.424 214	42.434 643
100.0	90.028 155		90.325 428		90.387 158		90.409 584	90.420 181

[a]Drake and Yan [17].
[b]Jones *et al.* [15].

third and fourth excited state are investigated here. The singlet-triplet splitting of the ionization energies is very small for the complete regime $0<B<100$ (see Fig. 2 where the solid and broken lines are indistinguishable).

3. The subspace $M=-3$ and even-zparity

The total energies for the singlet subspace are given in Table VI. Again the only values available in the literature for all five states listed are those for the atom in field-free space and the relative accuracy of our field-free data is at least 10^{-6}. The corresponding ionization energies are shown in Fig. 3. Similar to the above-discussed symmetry subspaces the ionization energies of the ground and first excited state increase monotonically with increasing field strength whereas avoided crossings in the intermediate regime of field strengths cause the ionization energy of the higher excited states to oscillate. For $B>0.2$ a.u. a strictly monotonous behavior is observed. Since for the lowest state of $^1(-3)^+$ symmetry the excited electron occupies a tightly bound orbital, the corresponding ionization energy of the $1^1(-3)^+$ state increases much more rapidly than those of the excited states $\nu^1(-3)^+$, $\nu=2-5$ (see Fig. 3).

Table VII provides the total energies of the corresponding triplet states. Our field-free energy values possess the same accuracy as discussed above. Additionally for strong fields there are a few values available in the literature to compare our data with: In Ref. [15] the ground and first two excited states of $^3(-3)^+$ symmetry have been investigated for a few field strengths. Similar to the above-discussed symmetries our energies are systematically variationally lower by an absolute value of $10^{-3}-10^{-4}$ a.u. than those given in Ref. [15]. Also the third and fourth excited states are investigated here. The singlet-triplet splitting of the ionization energies again is very small for the complete regime $0<B<100$ a.u. (see Fig. 3).

B. Electromagnetic transitions

1. General remarks

Analyzing observational spectra from magnetic cosmic objects and, in particular, magnetic white dwarfs requires extensive and accurate data on transitions among atomic energy levels. In the following we provide an overview of the electric dipole transitions that involve the above-discussed subspaces of symmetry. Specifically we address the behavior of the wavelengths as a function of the field strength $\lambda(B)$ in the regime $0<B<100$ a.u. Linear polarized transitions with the selection rules ($\Delta M=0$, $\Delta\Pi_z=\pm1$, $\Delta S=0$, $\Delta S_z=0$) are presented for the symmetry combinations $^{1/3}(-2)^+ \leftrightarrow {}^{1/3}(-2)^-$, where $^{1/3}$ indicates the spin singlet and triplet symmetry. Circular polarized transitions that obey the selection rules ($\Delta M=\pm1$, $\Delta\Pi_z=0$, $\Delta S=0$, $\Delta S_z=0$) are dis-

TABLE VI. Total energies E of the ground and first four excited singlet states $\nu^1(-3)^+$, $\nu=1-5$ as a function of the magnetic field strength B. The values for $B=0$ given in the literature are included. No values for finite field strength are available in the literature for comparison.

B	$E(1^1(-3)^+)$	$E(2^1(-3)^+)$	$E(3^1(-3)^+)$	$E(4^1(-3)^+)$	$E(5^1(-3)^+)$
0.000	−2.031 255	−2.020 003	−2.013 891	−2.013 889	−2.010 202
	−2.031 255 1[a]	−2.020 002 9[a]	−2.013 890 6[a]	−2.013 889 0[a]	−2.010 205[a]
0.0008	−2.032 429	−2.021 123	−2.015 006	−2.014 905	−2.011 192
0.004	−2.036 630	−2.024 176	−2.018 078	−2.016 111	−2.012 784
0.008	−2.040 901	−2.025 814	−2.019 958	−2.014 798	−2.012 586
0.020	−2.049 509	−2.025 607	−2.019 480	−2.011 883	−2.005 336
0.040	−2.056 966	−2.022 405	−2.008 882	−2.004 790	−1.997 514
0.080	−2.061 581	−2.011 702	−1.990 758	−1.980 089	−1.974 083
0.160	−2.054 993	−1.982 240	−1.954 396	−1.941 150	−1.933 977
0.240	−2.038 975	−1.948 003	−1.915 422	−1.900 585	−1.892 525
0.400	−1.992 916	−1.872 310	−1.833 001	−1.816 060	−1.806 885
0.500	−1.958 118	−1.821 744	−1.779 237	−1.761 350	−1.752 322
0.800	−1.835 926	−1.659 476	−1.609 746	−1.589 833	−1.580 004
1.0	−1.743 559	−1.544 293	−1.490 917	−1.470 031	−1.459 860
1.6	−1.430 317	−1.173 373	−1.111 909	−1.088 966	−1.078 020
2.0	−1.199 054	−0.909 469	−0.843 996	−0.820 079	−0.808 779
5.0	0.843 450	1.311 628	1.394 377	1.422 224	1.434 804
10.0	4.783 783	5.447 132	5.543 427	5.574 111	5.587 684
20.0	13.371 608	14.297 681	14.407 614	14.440 991	14.455 609
50.0	40.842 417	42.249 754	42.377 579	42.414 286	42.429 703
100.0	88.317 766	90.218 478	90.359 625	90.398 689	90.415 190

[a]Drake and Yan [17].

cussed for the combinations $^{1/3}(-3)^+ \leftrightarrow {}^{1/3}(-2)^+$, $^{1/3}(-2)^+ \leftrightarrow {}^{1/3}(-1)^+$, $^{1/3}(-2)^- \leftrightarrow {}^{1/3}(-1)^-$. These transitions are complementary to those discussed previously in Refs. [9, 10] and therefore provide essential new information on the spectral properties of the helium atom in a strong magnetic field. The total number of transitions investigated here is of the order of 250. So far only the situation $M \leqslant 0$ has been mentioned. The transition energies for $M \geqslant 0$ can, however, easily be obtained from the data for $M \leqslant 0$ by performing the following shift:

$$E(-M_f) - E(-M_i) = E(M_f) - E(M_i) - B(M_f - M_i), \tag{13}$$

where i/f labels the initial and final states, respectively. Particularly for $M_i = M_f$ the transition energies (wavelengths) are identical for both the states with positive and negative magnetic quantum numbers. From an astronomical point of view the transitions involving states with positive magnetic quantum numbers are of less interest since they are highly excited and in general do not exhibit additional stationarities as a function of the field strength (see below).

2. Transition spectra

Figure 4(a) illustrates the wavelengths belonging to the 50 circular polarized transitions $\nu^1(-1)^+ \rightarrow \mu^1(-2)^+$ for $\nu = 1-10$, $\mu = 1-5$ for the complete regime of field strengths investigated in the present work. Here and in the following the smooth curves have been obtained from our grid of energies for 20 values of the field strength by a sophisticated interpolation procedure. The interpolation error is in most cases estimated to be significantly smaller than the accuracy of our transition energies. Apart from the higher excitations $\nu > 5$, only in a small number of cases the necessary convergence could not be achieved and, consequently, the corresponding curves $\lambda(B)$ do not cover the complete interval $0 < B < 100$ a.u. but end at some field strength $B_c < 100$ a.u. The singlet transitions in Fig. 4(a) show a number of eye-catching features. First of all there is a bundle of transitions with short wavelengths that is for strong fields separated from the wavelengths of the remaining transitions. The wavelength of the center of this bundle decreases in the high-field regime strongly with increasing field strength. This bundle is associated with the fact that both electrons occupy, in at least one of the states involved in the transitions, tightly bound orbitals. Since for helium the bound-state spectrum consists exclusively of one-particle excitations, one electron always occupies the ''core'' orbital $1s$ which is the most tightly bound orbital. The above statement therefore essentially means that the second excited electron also occupies a tightly bound orbital. In the case of Fig. 4(a) this can be the $2p_{-1}$, $3d_{-2}$ orbitals. Indeed, a careful look at Fig. 4(a) reveals that there are two closely neighbored bundles with short wavelengths. Furthermore, we clearly see the strong oscillatory behavior of the transition wavelengths in the intermediate regime of field strengths that corresponds to the regime of avoided crossings for the total or ionization energies (see Sec. III A). It is this regime which is, from a con-

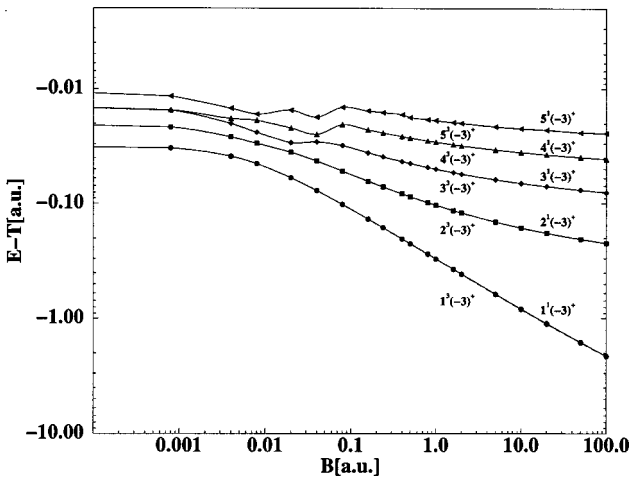

FIG. 3. The ionization energies of the ground and first four excited states $\nu^{2S+1}(-3)^+$ for both singlet ($S=0$) (solid lines) and triplet ($S=1$) (broken lines) symmetry as a function of the field strength. In the considered range of field strengths the singlet-triplet splitting is very small. Both energies and field strengths are given in atomic units.

ceptual point of view, the most difficult to describe since the wave function is strongly distorted and does not show any approximate symmetries that typically occur in the weak- or high-field situation. Due to this restructuring of the wave function and the fact that different exact symmetries are involved in the transitions, we particularly also encounter exact level crossings that lead to singularities with respect to the transition wavelengths [see Fig. 4(a)]. From the above it is clear that most of the stationarities with respect to $\lambda(B)$ occur in the intermediate regime. The latter are of particular importance for the interpretation of the spectra of white dwarfs possessing a strong field. Figure 4(a) shows also that in the high-field limit a reordering due to the evolution of the Landau zonal structure takes place. Interestingly the phenomenon of the increase of the ionization energies for the excited $^1(-2)^+$ states for fields close to 100 a.u. (see Fig. 1 and the discussion in Sec. III A) reflects itself clearly for the transition wavelengths illustrated in Fig. 4(a): There are severe changes (and singularities) of the corresponding transition wavelengths close to $B\approx 100$ a.u. Within the presently discussed symmetries this phenomenon is exclusively associated with the subspace $^1(-2)^+$ [see also Figs. 6(a) and 7(a)].

Figure 4(b) provides the transition wavelengths as a function of the field strength for the corresponding triplet states, i.e., $\nu^3(-1)^+ \rightarrow \mu^3(-2)^+$ for $\nu=1-10$, $\mu=1-5$. The overall picture is similar to the one given for the singlet states in Fig. 4(a) i.e., many of the statements given there hold also for the triplet states but there are also a number of significant differences due to, e.g., a different level-crossing

TABLE VII. Total energies E of the ground and first four excited triplet states $\nu^3(-3)^+$, $\nu=1-5$ as a function of the magnetic field strength B. The best values $E_{\rm lit}$ available in the literature are included for comparison. For the third and fourth excited state only the energy values for $B=0$ are known so far.

	$1^3(-3)^+$		$2^2(-3)^+$		$3^3(-3)^+$		$4^3(-3)^+$	$5^3(-3)^+$
B	E	$E_{\rm lit}$	E	$E_{\rm lit}$	E	$E_{\rm lit}$	E	E
0.000	−2.031 255	−2.031 255 1[a]	−2.020 003	−2.020 002 9[a]	−2.013 891	−2.013 890 6[a]	−2.013 889	−2.010 202
							−2.013 889 0[a]	−2.010 205[a]
0.0008	−2.032 429		−2.021 123		−2.015 006		−2.014 905	−2.011 192
0.004	−2.036 630		−2.024 176		−2.018 078		−2.016 111	−2.012 784
0.008	−2.040 901		−2.025 814		−2.019 958		−2.014 798	−2.012 586
0.020	−2.049 509		−2.025 607		−2.019 480		−2.011 883	−2.005 336
0.040	−2.056 967		−2.022 405		−2.008 883		−2.004 790	−1.997 514
0.080	−2.061 582	−2.0606[b]	−2.011 702	−2.0114[b]	−1.990 758	−1.9851[b]	−1.980 089	−1.974 084
0.160	−2.054 999		−1.982 241		−1.954 896		−1.941 150	−1.933 977
0.240	−2.038 994		−1.948 006		−1.915 424		−1.900 586	−1.892 526
0.400	−1.992 988	−1.9923[b]	−1.872 322	−1.8721[b]	−1.833 006	−1.8320[b]	−1.816 062	−1.806 887
0.500	−1.958 243		−1.821 762		−1.779 243		−1.761 353	−1.752 323
0.800	−1.836 282	−1.8344[b]	−1.659 521	−1.6587[b]	−1.609 760	−1.6085[b]	−1.589 839	−1.580 007
1.0	−1.744 109		−1.544 357		−1.490 936		−1.470 039	−1.459 864
1.6	−1.431 517	−1.4275[b]	−1.173 488	−1.1726[b]	−1.111 942	−1.1110[b]	−1.088 980	−1.078 027
2.0	−1.200 682		−0.909 609		−0.844 035		−0.820 094	−0.808 788
5.0	0.839 445		1.311 425		1.394 328		1.422 205	1.434 794
10.0	4.777 598		5.446 941		5.543 384		5.574 095	5.587 676
20.0	13.363 039		14.297 510		14.407 571		14.440 973	14.455 599
50.0	40.830 300		42.249 430		42.377 448		42.414 226	42.429 671
100.0	88.302 575		90.217 437		90.359 091		90.398 425	90.415 021

[a]Drake and Yan [17].
[b]Jones *et al.* [15].

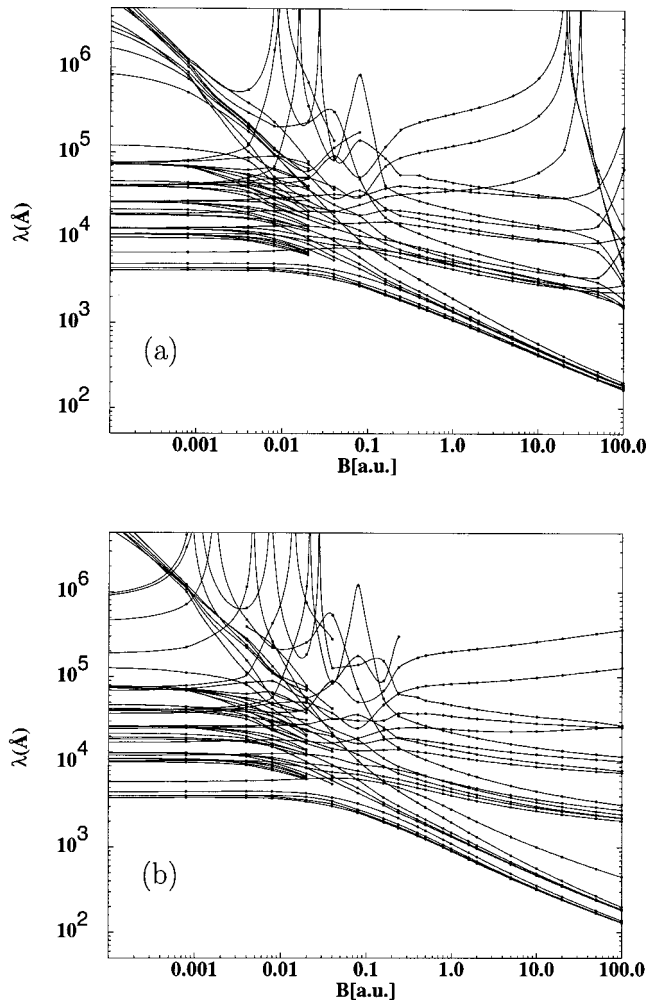

FIG. 4. (a) The transition wavelengths (in Å) of the singlet ($|\Delta M|=1$) transitions $\nu^1(-1)^+ \rightarrow \mu^1(-2)^+$ for $\nu=1-10$, $\mu=1-5$ as a function of the field strength (in atomic units). (b) The transition wavelengths of the triplet ($|\Delta M|=1$) transitions $\nu^3(-1)^+ \rightarrow \mu^3(-2)^+$ for $\nu=1-10$, $\mu=1-5$ as a function of the field strength.

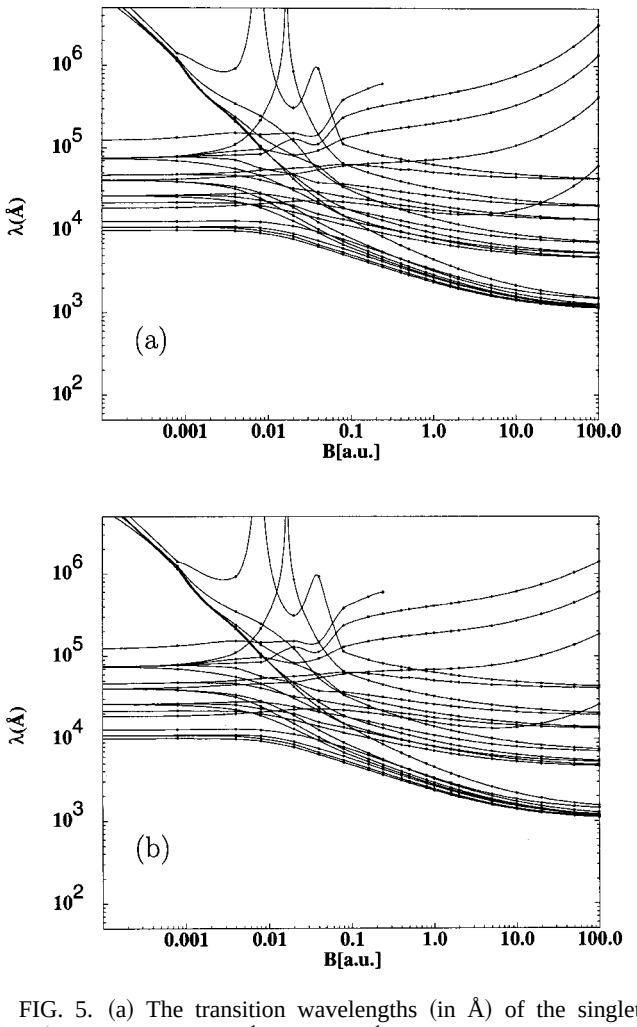

FIG. 5. (a) The transition wavelengths (in Å) of the singlet ($|\Delta M|=1$) transitions $\nu^1(-1)^- \rightarrow \mu^1(-2)^-$ for $\nu=1-5$, $\mu=1-5$ as a function of the field strength (in atomic units). (b) The transition wavelengths of the triplet ($|\Delta M|=1$) transitions $\nu^3(-1)^- \rightarrow \mu^3(-2)^-$ for $\nu=1-5$, $\mu=1-5$ as a function of the field strength.

pattern and the missing energy lowering in the high-field regime for the excited triplet $^3(-2)^+$ states compared to the singlet ones.

Figures 5(a) and 5(b) show the behavior of the transition wavelengths for the 50 singlet and triplet circular polarized transitions $\nu^{1/3}(-1)^- \rightarrow \mu^{1/3}(-2)^-$ for $\nu=1-5$, $\mu=1-5$, respectively. First of all we realize that the two pictures are very similar, i.e., the difference between the singlet and triplet wavelengths is small compared to the energetic resolution of Fig. 5. For weak and high fields the transition curves form a few bundles that correspond to the higher symmetries, i.e., the near degeneracies in these cases. It is worth while to note that, opposite to the previously considered transitions in Figs. 4(a) and 4(b) there are no bundles that show a strongly decreasing wavelength of their centers in the high-field situation. This is because there is no tightly bound orbital available for the excited electron in the case of the symmetries $(-2)^-$ and $(-1)^-$. A new feature of the singlet and triplet transitions shown in Figs. 5(a) and 5(b) compared to the transitions in Figs. 4(a) and 4(b) is the occurence of a few transitions that are energetically well separated and, more importantly, whose wavelengths increase significantly for strong fields [these are the four upwards turning curves in Figs. 5(a) and 5(b) for $B \geqslant 1.0$]. This is due to the fact that the energies of the $\nu(-1)^-$ states increasingly approach those of the $\nu(-2)^-$ states both for singlet and triplet symmetry.

Figures 6(a) and 6(b) illustrate the transition wavelengths for the 50 singlet and triplet linear polarized transitions $\nu^{1/3}(-2)^+ \rightarrow \mu^{1/3}(-2)^-$ for $\nu=1-5$, $\mu=1-5$, respectively. Apart from the high-field behavior that yields, in particular, additional exact level crossings for the singlet states, the two pictures are very similar. We have a single bundle of transitions with short wavelengths that decreases monotonically with increasing field strength. This bundle is due to the tightly bound orbital $3d_{-2}$ which occurs for the lowest $^{1/3}(-2)^+$ configuration. Many of the explanations given for Fig. 4(a) are valid here also.

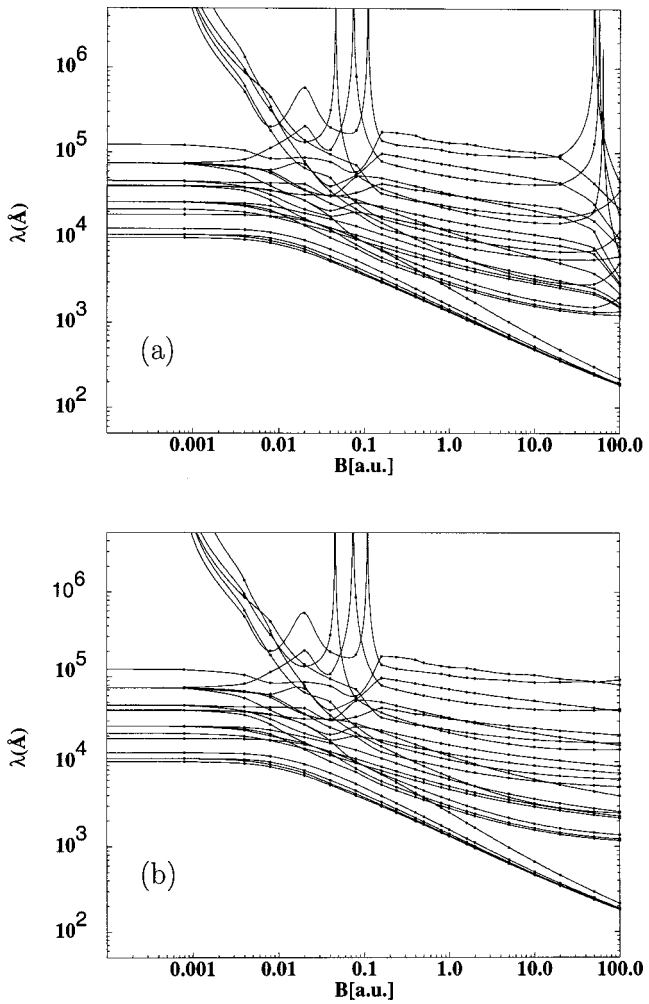

FIG. 6. (a) The transition wavelengths (in Å) of the singlet ($|\Delta M|=0$) transitions $\nu^1(-2)^+ \rightarrow \mu^1(-2)^-$ for $\nu=1-5$, $\mu=1-5$ as a function of the field strength (in atomic units). (b) The transition wavelengths of the triplet ($|\Delta M|=0$) transitions $\nu^3(-2)^+ \rightarrow \mu^3(-2)^-$ for $\nu=1-5$, $\mu=1-5$ as a function of the field strength.

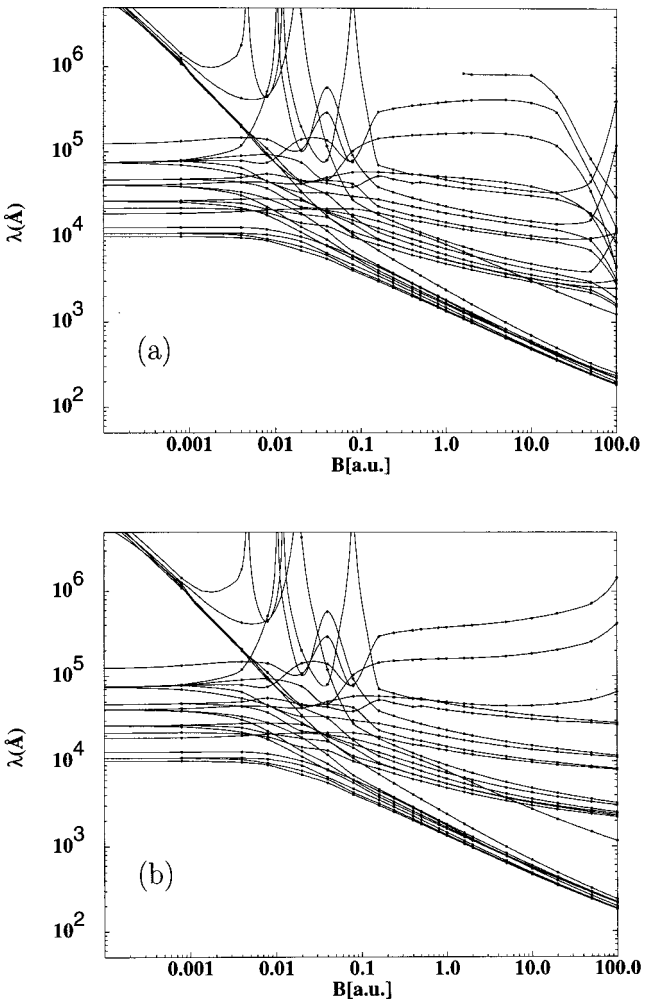

FIG. 7. (a) The transition wavelengths (in Å) of the singlet ($|\Delta M|=1$) transitions $\nu^1(-2)^+ \rightarrow \mu^1(-3)^+$ for $\nu=1-5$, $\mu=1-5$ as a function of the field strength (in atomic units). (b) The transition wavelengths of the triplet ($|\Delta M|=1$) transitions $\nu^3(-2)^+ \rightarrow \mu^3(-3)^+$ for $\nu=1-5$, $\mu=1-5$ as a function of the field strength.

Finally Figs. 7(a) and 7(b) show the transition wavelengths for the 50 singlet and triplet circular polarized transitions $\nu^1(-2)^+ \rightarrow \mu^1(-3)^+$ for $\nu=1-5$, $\mu=1-5$, respectively. Since the $^1(-2)^+$ subspace is involved in the transitions shown in Fig. 7(a), the high-field limit $B \approx 100$ a.u. shows the same peculiarities as discussed above. This also represents the major difference between the singlet [Fig. 7(a)] and triplet [Fig. 7(b)] transition curves. Two bundles of short-wavelength transitions can be observed due to the fact that the two tightly bound orbitals $3d_{-2}$, $4f_{-3}$ are involved in the corresponding transitions.

For all transitions among the considered subspaces (see Figs. 4–7) a bundle of transition curves with very large wavelengths for weak magnetic fields $B \leqslant 0.01$ a.u. occurs. The wavelengths of the centers of these bundles decrease strongly with increasing field strength. For the limit case of a vanishing field strength the corresponding transition wavelengths remain finite but are very large. The reason for this is as follows. Without electron-electron interaction certain states with different total angular momenta L arising from the same one-particle excitation shell are degenerate. For highly excited states of the helium atom the electron-electron interaction is weak and therefore these states show a small energetic splitting. With increasing field strength this split increases significantly (the approximate degeneracy is lifted) and that is exactly what we are observing for the above bundle of transitions. The above arguments hold in particular for the linear polarized transitions $\Delta M=0$. For the circular polarized transitions $\Delta M=-1$ the Zeeman splitting adds to the above-mentioned energetical splitting and a slightly different behavior of the corresponding bundles of transition wavelengths is observed.

3. Stationary transition points

The field configuration of magnetic white dwarfs is typically a dipole configuration, which means that the field strength varies by a factor of 2 from the pole to the equator.

Transitions that behave monotonically as a function of the varying field are smeared out, i.e., are not expected to provide a signature in the observed spectrum. However, the transitions whose wavelengths are stationary with respect to the field dependence manifest themselves as absorption edges in the observable spectrum if they possess a relevant intensity. This argument is particularly valid in the strong field situation. A list of stationary transitions, including their wavelengths, their positions with respect to the field strength, as well as their character (maximum, minimum), is therefore a key ingredient for a comparison of theory and observation. In the astronomically relevant regime of wavelengths $\lambda \leqslant 300\,00$ Å we found 94 stationarities. A complete list of stationarities like any other data of the present investigation can be obtained from the authors upon request. Remarkably only a very few of the stationary transitions obtained here add to the ones relevant to the analysis of the magnetic white dwarf GD229 [14]. Finally we remark that finite nuclear mass corrections can be included via scaling relations. We refer the reader herefore to Refs. [2,10,16].

IV. CONCLUSIONS AND OUTLOOK

In the present work we have investigated higher excited angular-momentum states of the helium atom for the complete regime of field strengths $0<B<100$ a.u. Total and ionization energies as well as the electromagnetic transition wavelengths have been studied and discussed in detail for spin singlet and triplet symmetry for both gerade and ungerade z parity and for the magnetic quantum numbers $M=\pm 2,\pm 3$. This complements our overall picture of the energetics of the atom obtained in previous investigations [9,10]. Particularly, an enhanced list of stationary transitions that are relevant to the identification of spectra emerging from magnetic white dwarf is now available.

Our extensive study of the helium atom in strong magnetic fields was possible by using a basis set of anisotropic Gaussian one-particle functions that are particularly adapted to the anisotropy in the presence of the external field. A careful optimization of the nonlinear variational parameters for each field strength is essential for the rapid convergence of the variational results to the exact ones. Although this optimization procedure was originally a tedious work we succeeded very recently in developing a number of tools that automatize it to some extent and, in particular, allows it to avoid linear dependencies of the nonorthogonal basis functions. These new tools are currently being applied [18].

Estimated accuracies of $10^{-4}-10^{-6}$ for the total energies of the electronic states of the helium atom could be achieved this way for arbitrary field strength using a full configuration-interaction approach. From a computational point of view the key ingredient to a fast buildup of the Hamiltonian matrix is certainly the rapid evaluation of the electron-electron integrals. Using a combination of advanced analytical and coding techniques we could drastically reduce the typical CPU necessary, thereby making a series production of data possible. Most of the excited states presented in this work have not been investigated in the literature so far.

The ionization and transition energies clearly reflect the increasing spectral complexity with an increasing degree of excitation that arises due to the large number of avoided and exact crossings, especially in the intermediate regime of field strengths. The dominant features of the behavior of the energies could be explained and assigned to, for example, tightly bound orbitals, correlation effects, level-crossing structures, etc.

Clearly in order to go beyond the pure energetics of the atom it is now necessary to calculate the oscillator strengths of the electromagnetic transitions investigated so far. This is highly desirable also from an astrophysical point of view since the ultimate goal is to solve the corresponding radiation transport equations for the atmosphere which then yield synthetic spectra. To this end, however, further conceptual programming work is necessary which is mainly due to the complicated I/O involved and the assignment of eigenvectors resulting from different calculations to the proper two-particle configurations. Oscillator strengths will therefore be presented in a future work.

ACKNOWLEDGMENTS

The Deutsche Forschungsgemeinschaft is gratefully acknowledged for financial support. We thank H. D. Meyer for fruitful discussions.

[1] H. Friedrich, Phys. Rev. A **26**, 1827 (1982).
[2] H. Ruder, G. Wunner, H. Herold, and F. Geyer, *Atoms in Strong Magnetic Fields* (Springer-Verlag, Berlin, 1994).
[3] W. Rösner, G. Wunner, H. Herold, and H. Ruder, J. Phys. B **17**, 29 (1984).
[4] D. Wintgen and H. Friedrich, J. Phys. B **19**, 991 (1986).
[5] M. V. Ivanov, J. Phys. B **21**, 447 (1988).
[6] Yu. P. Kravchenko, M. A. Liberman, and B. Johansson, Phys. Rev. A **54**, 287 (1996).
[7] *Atoms and Molecules in Strong External Fields*, edited by P. Schmelcher and W. Schweizer (Plenum, New York, 1998).
[8] Usually it is assumed that only the lightest elements like hydrogen and helium can occur in the atmospheres of isolated magnetic white dwarfs. However, recently it has been pointed out (J. Liebert, private communication) that certain magnetic white dwarfs can accrete interstellar matter which leads to the presence of a variety of heavier elements in their atmospheres. It is expected that such objects are very frequent.
[9] W. Becken, P. Schmelcher, and F. K. Diakonos, J. Phys. B **32**, 1557 (1999).
[10] W. Becken and P. Schmelcher, J. Phys. B **33**, 545 (2000).
[11] R. F. Green and J. Liebert, Publ. Astron. Soc. Pac. **93**, 105 (1980).
[12] G. D. Schmidt, W. B. Latter, and C. B. Foltz, Astrophys. J. **350**, 758 (1990).
[13] G. D. Schmidt, R. G. Allen, P. S. Smith, and J. Liebert, Astrophys. J. **463**, 320 (1996).
[14] S. Jordan, P. Schmelcher, W. Becken, and W. Schweizer, As-

tron. Astrophys. **336**, L33 (1998).
[15] M. D. Jones, G. Ortiz, and D. M. Ceperley, Phys. Rev. A **59**, 2875 (1999).
[16] V. B. Pavlov-Verevkin and B. I. Zhilinskii, Phys. Lett. **78A**, 244 (1980).
[17] G. W. F. Drake and Z.-C. Yan, Phys. Rev. A **46**, 2378 (1992); Chem. Phys. Lett. **229**, 486 (1994).
[18] O. A. Al-Hujaj and P. Schmelcher, Phys. Rev. A **61**, 052512 (2000); and (unpublished).